JHEP|Reports

Microcystin-RR is a biliary toxin selective for neonatal extrahepatic cholangiocytes

Authors

Kapish Gupta, Dongning Chen, Rebecca G. Wells

Correspondence

rgwells@pennmedicine.upenn.edu (R.G. Wells).

Graphical abstract

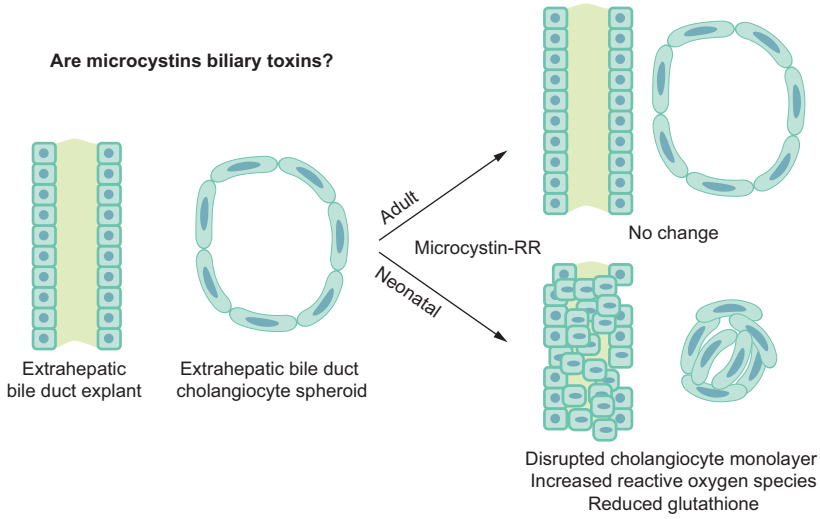

Microcystin-RR, but not other microcystins, is a neonatal extrahepatic cholangiocyte toxin

Highlights:

- Neonatal but not adult EHBD cholangiocytes showed damage in the presence of 400 nM microcystin-RR.
- These neonatal EHBD cholangiocytes did not show damage in response to six other microcystins tested.
- Neonatal extrahepatic bile ducts are likely to have immature antioxidant defense systems.

Impact and implications:

The plant toxin biliatresone causes a biliary atresia-like disease in livestock and vertebrate animal model systems. We tested the widespread blue-green algal toxin, microcystin-RR, another highly electrophilic unsaturated carbonyl compound that is released during harmful algal blooms, and found that it was also a biliary toxin with specificity for neonatal extrahepatic cholangiocytes. This work should drive further animal studies and, ultimately, studies to determine whether human exposure to microcystin-RR causes biliary atresia.

https://doi.org/10.1016/j.jhepr.2024.101218

JHEP|Reports

Microcystin-RR is a biliary toxin selective for neonatal extrahepatic cholangiocytes

Kapish Gupta[1,2,†], Dongning Chen[1,2,3], Rebecca G. Wells[1,2,3,*]

JHEP Reports **2025**. vol. 7 | 1–12

Background & Aims: Biliary atresia is a fibrosing cholangiopathy affecting neonates that is thought to result from a prenatal environmental insult to the bile duct. Biliatresone, a plant toxin with an α-methylene ketone group, was previously implicated in biliary atresia in Australian livestock, but is found in a limited location and is unlikely to be a significant human toxin. We hypothesized that other unsaturated carbonyl compounds, some with the potential for significant human exposure, might also be biliary toxins.

Methods: We focused on the family of microcystins, cyclic peptide toxins from blue-green algae that are found worldwide, particularly during harmful algal blooms. We used primary extrahepatic cholangiocyte spheroids and extrahepatic bile duct explants from both neonatal [a total of 86 postnatal day (P) 2 mouse pups and 18 P2 rat pups (n = 8–10 per condition for both species)] and adult rodents [a total of 31 P15–18 mice (n = 10 or 11 per condition)] to study the biliary toxicity of microcystins and potential mechanisms involved.

Results: Results showed that 400 nM microcystin (MC)-RR, but not six other microcystins or the related algal toxin nodularin, caused >80% lumen closure in cell spheroids made from extrahepatic cholangiocytes isolated from 2–3-day-old mice (p <0.0001). By contrast, 400 nM MC-RR resulted in less than an average 5% lumen closure in spheroids derived from neonatal intrahepatic cholangiocytes or cells from adult mice (p = 0.4366). In addition, MC-RR caused occlusion of extrahepatic bile duct explants from 2-day-old mice (p <0.0001), but not 18-day-old mice. MC-RR also caused a 2.3-times increase in reactive oxygen species in neonatal cholangiocytes (p <0.0001), and treatment with *N*-acetyl cysteine partially prevented microcystin-RR-induced lumen closure (p = 0.0004), suggesting a role for redox homeostasis in its mechanism of action.

Conclusions: We identified MC-RR as a selective neonatal extrahepatic cholangiocyte toxin and suggest that it acts by increasing redox stress.

Introduction

Biliary atresia (BA) is a potentially fatal disease of neonates. It is a fibrosing cholangiopathy that is diagnosed within the first months of life but is thought to result from a prenatal environmental insult that damages the fetal extrahepatic bile duct (EHBD), causing duct obstruction and, ultimately, end-stage liver disease. BA occurs in 1:3,500–1:19,000 live births worldwide; it is one of the most important pediatric liver diseases and the major indication for liver transplant in children in the USA.[1–4] Importantly, BA is never seen in older children or in the mothers of affected babies, suggesting a developmental susceptibility to the as-yet-unknown exposure.[3] The disease is characterized by progressive inflammation, fibrosis, and obstruction of the bile ducts, resulting in extrahepatic duct obliteration with impaired bile flow, cholestasis, and fibrosis.[5] Despite advances in medical and surgical management, care of patients with BA remains a significant challenge, and early diagnosis and intervention are crucial to improving outcomes and preventing long-term complications.[6,7]

Although candidate genetic modifiers have been identified, BA is not a genetic disease and epidemiological data suggest that prenatal environmental insults, such as viral infections and toxin exposure, are primary causes.[8–11] However, despite extensive study, only a small percentage of BA cases have been linked to viral infections, primarily cytomegalovirus,[12] while the insult in most cases remains unknown.

A plant toxin, biliatresone, was previously identified as a likely cause of a BA-like disease in Australian livestock.[9] Biliatresone is toxic to the extrahepatic bile ducts (EHBDs) of larval zebrafish and to mammalian cholangiocytes *in vitro* and can cause a BA-like phenotype in mouse pups.[13–17] It is highly electrophilic and has an α-methylene ketone group that can form adducts with cysteine residues in proteins, affecting redox metabolism.[18] Several lines of evidence implicate redox stress in neonatal EHBD damage: the EHBDs of neonates have low levels of reduced glutathione (GSH) at baseline; artificially lowering GSH causes damage to cholangiocyte spheroids and neonatal EHBD explants; and *N*-acetyl cysteine (NAC) treatment protects against damage from biliatresone.[13,19]

Although it is highly unlikely that pregnant women are exposed to biliatresone, these findings suggest that toxin exposure and redox stress during prenatal development contribute to the development of BA. We hypothesized that environmental toxins that are unsaturated (electrophilic)

* Corresponding author. Address: 421 Curie Boulevard, 905 BRB II/III, Philadelphia, PA 19104, USA. Tel.: +1-610-322-2627; Fax: +1-215-573-2024.
E-mail address: rgwells@pennmedicine.upenn.edu (R.G. Wells).
† Current address: Department of Biosciences and Bioengineering, Indian Institute of Technology, Guwahati, Assam, India.
https://doi.org/10.1016/j.jhepr.2024.101218

carbonyl compounds, such as biliatresone, might also be biliary toxins. The 250+ toxins in the microcystin family, which are found worldwide, are alpha-acylamino-alpha-methylene-amides and are particularly attractive biliary toxin candidates. They are cyclic heptapeptides with L-amino acid residues at positions 2 and 4 (Fig. 1A); microcystin-LR (leucine-arginine; MC-LR) is the most prominent congener and MC-RR (arginine-arginine) the second most commonly identified.[20–22] These microcystins are potent hepatotoxins produced by various species of cyanobacteria (often *Microcystis* species), which occur commonly as part of harmful algal blooms in freshwater ecosystems worldwide.[23] They are a significant threat to public health, accumulating in aquatic organisms, such as fish and shellfish, and entering the human food chain.[24] In addition,

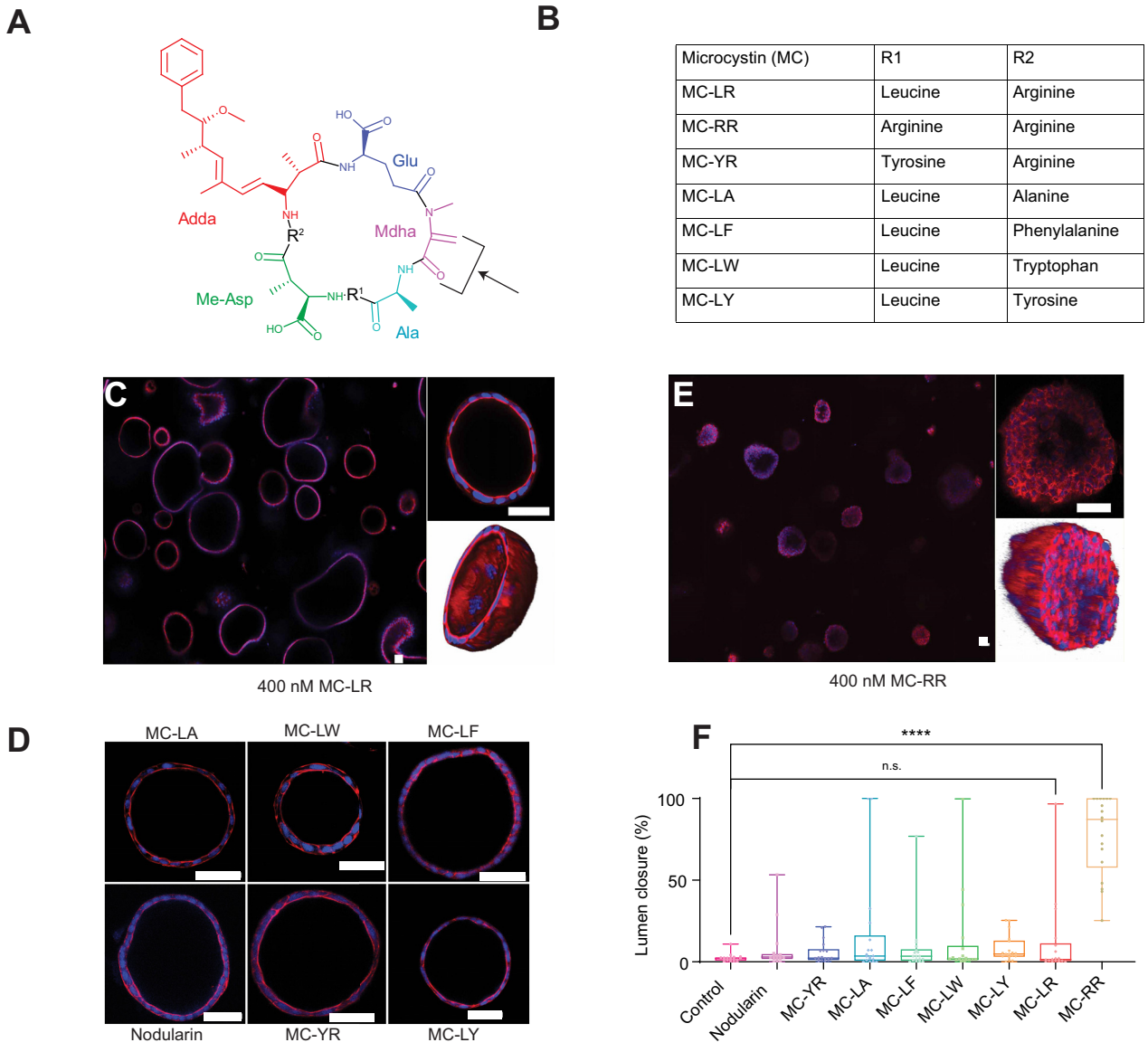

Microcystin (MC)	R1	R2
MC-LR	Leucine	Arginine
MC-RR	Arginine	Arginine
MC-YR	Tyrosine	Arginine
MC-LA	Leucine	Alanine
MC-LF	Leucine	Phenylalanine
MC-LW	Leucine	Tryptophan
MC-LY	Leucine	Tyrosine

Fig. 1. Microcystin (MC)-RR treatment results in neonatal extrahepatic bile duct (EHBD) cholangiocyte spheroid damage. (A) General structure of MCs showing the cyclic heptapeptide backbone with two variable amino acid groups (marked as R^1 and R^2). The proposed active group, based on similarity to biliatresone, is highlighted by arrow. (B) Commercially available MCs tested, with the identity of amino acids at R^1 and R^2 noted. (C) Neonatal EHBD cholangiocyte spheroids forming one cell-thick hollow spheroids that are unchanged in the presence of 400 nM MC-LR. The middle section of a representative spheroid is highlighted and the 3D rendering shows a typical hollow lumen. (D) Neonatal EHBD cholangiocyte spheroids similarly form one cell-thick hollow spheroids with open lumens after treatment with 400 nM of various MCs or nodularin for 24 h. (E) Neonatal EHBD cholangiocyte spheroids demonstrate filled lumens after treatment with 400 nM MC-RR for 24 h. The middle section of a representative spheroid is highlighted and the 3D rendering shows the lumen filled with cells. (F) Quantification of lumen closure in the presence of all the tested MCs and nodularin: $p = 0.9726$, control *vs*. nodularin; $p = 0.9968$, control *vs*. MC-YR; $p = 0.1501$, control *vs*. MC-LA; $p = 0.9317$, control *vs*. MC-LF; $p = 0.5087$, control *vs*. MC-LW; $p = 0.9373$, control *vs*. MC-LY; $p = 0.9373$, control *vs*. MC-LR; $p = <0.0001$, control *vs*. MC-RR. Statistical significance determined using one-way ANOVA followed by multiple comparison with control and correction using Dunnett's method, where: $^*p \leq 0.05$, $^{**}p \leq 0.01$, $^{***}p \leq 0.001$, and $^{****}p \leq 0.0001$. All images are representative of a minimum of 18 spheroids in total for each condition, derived from three independent experiments, quantified for lumen closure. Control spheroids were vehicle treated. Red indicates actin, blue indicates DAPI. Scale bars: 50 μm. Adda, (all-S,all-E)-3-amino-9-methoxy-2,6,8-trimethyl-10-phenyldeca-4,6-dienoic acid; Ala, alanine; Glu, glutamic acid; Mdha, *N*-methyldehydroalanine; Me-Asp, D-erythro-β-methyl-isoaspartic acid.

exposure to microcystins can occur through recreational activities, such as swimming and boating, as well as through drinking water contaminated with cyanobacteria.[25]

In this study, we evaluated the toxicity of seven commercially available microcystins (Fig. 1B) and a related cyanobacterial toxin, nodularin, on primary mouse and rat cholangiocytes and EHBD explants. We compared the effects of the different toxins on neonatal *vs*. adult cells and tissues, and identified a partial mechanism of action for MC-RR, the one microcystin found to be toxic in our study. Our results suggest that MC-RR should be investigated as a cause of human BA.

Materials and methods

Reagents

Microcystins were obtained from Enzo Life Sciences (Farmingdale, NY, USA) and Cayman Chemical Company (Ann Arbor, MI, USA). The Microcystin (Adda-specific) ELISA kit was purchased from Enzo Life Sciences. Pranlukast (P0080), thiazolyl blue tetrazolium bromide (M2128), suramin sodium salt (S2671), and NAC (A9165) were from Sigma (Burlington, MA, USA). Rat tail collagen (354236) and Matrigel (354234) were from Corning (Corning, NY, USA). The TUNEL assay kit (C10247) and CellRox Green (C10444) were obtained from Invitrogen (Waltham, MA, USA). A list of antibodies and dyes used in the study can be found in Table S1.

Experimental animals

BALB/c mice [postnatal day (P)2–3, P15–18, and adult] and Sprague–Dawley rats (CD IGS, P2–3) were used in this study. Animals were euthanized and EHBDs were isolated and used either in cell culture or for direct experimentation, as described in the Supplementary material. All animal experiments were performed in accordance with National Institutes of Health policy and were approved by the Institutional Animal Care and Use Committee of the University of Pennsylvania (Protocol number: 804862). We did not determine sex given that anogenital distance measurements at P2 lack accuracy, but our random selection of pups typically yielded a balanced male–female distribution. Each batch of primary cells was isolated from 8–10 pups, and EHBD explants were isolated from pups (8–14 per condition, per experiment) chosen randomly.

Spheroid culture

Cholangiocytes were isolated by outgrowth from the EHBDs of neonatal (P2–3) or adult mice, as described elsewhere.[26] Isolated cells were cultured either on collagen-coated dishes or in 3D in a collagen-Matrigel mixture.[15] Cholangiocytes in the collagen-Matrigel mixture formed spheroids within 5 days and were used for experiments 6–8 days after plating. EHBDs in collagen and cholangiocytes were cultured in biliary epithelial cell (BEC) media as described elsewhere,[26] with the exception that the final serum concentration was 10%. The media was changed every 2 days. During toxin treatment, the media was replaced with BEC media devoid of serum (referred to as 0% BEC media). Microcystin treatment time was 24 h unless otherwise noted. Following treatments, spheroids were fixed and stained as described in the Supplementary material. Microcystin stocks were prepared using ethanol, and a 0.1% ethanol solution served as the vehicle control consistently throughout the study. There was no difference in vehicle control and untreated samples.

Explant culture

Intact EHBDs from P2 mice, P15–18 mice, or P2 rats were cultured at 37 °C in 95% O_2/5% CO_2 in a Vitron Dynamic Organ Culture Incubator for 24 h in the presence of vehicle or a toxin. Ducts were stained as described previously[27] using antibodies against KRT19 and vimentin, and counterstained with DAPI (Supplementary material).

Image analysis

All samples were imaged using a water immersion 25 × objective lens on a Leica TCS SP8 confocal microscope. Z-stacks (at a distance of 5 μm) were obtained for spheroids and EHBDs. Spheroids were analyzed using a custom-made algorithm with ImageJ (Fig. S1). EHBD images were stitched together and are shown here with respect to the base stack (Fig. S2). EHBDs were scored as normal, partially damaged, or completely damaged as per the scoring method described in Fig. S3.

Statistical analysis

Statistical significance was calculated by either the one-tailed Student *t* test or one-way ANOVA followed by Tukey's test for *post hoc* analysis. Differences were significant at $p \leq 0.05$ (*), $p \leq 0.01$ (**), $p \leq 0.001$ (***), and $p \leq 0.0001$ (****).

Additional methods are provided in the Supplementary material.

Results

MC-RR damages neonatal cholangiocytes in spheroid culture

Cholangiocytes isolated from EHBDs can self-organize into polarized spheroids with hollow lumens (Fig. S4A). The morphology of spheroids generated from neonatal mouse cholangiocytes was unchanged compared with vehicle-treated control spheroids in the presence of nodularin and most of the microcystins tested, indicating their low toxicity in this system (Fig. 1C, D and F; Fig. S4E). However, exposure to 400 nM MC-RR resulted in loss of the spheroid monolayer and lumen closure (Fig. 1E and F), as assessed by a novel metric to quantitatively measure lumen closure; this was used for all lumen closure measurements throughout (Fig. S1). MC-RR-induced lumen closure was concentration dependent (average lumen closure of 83.7% in the presence of 400 nM MC-RR), with higher concentrations resulting in greater damage (Fig. 2A and B). MC-RR exposure also caused a loss of polarity, as evidenced by a significant decrease in the apical:basal actin ratio (Fig. 2C; Fig. S4). In contrast to these findings with neonatal EHBD cholangiocytes, spheroids derived from neonatal intrahepatic bile duct (IHBD) cholangiocytes or adult EHBD cholangiocytes showed no damage in the presence of MC-RR (Fig. 2D–G).

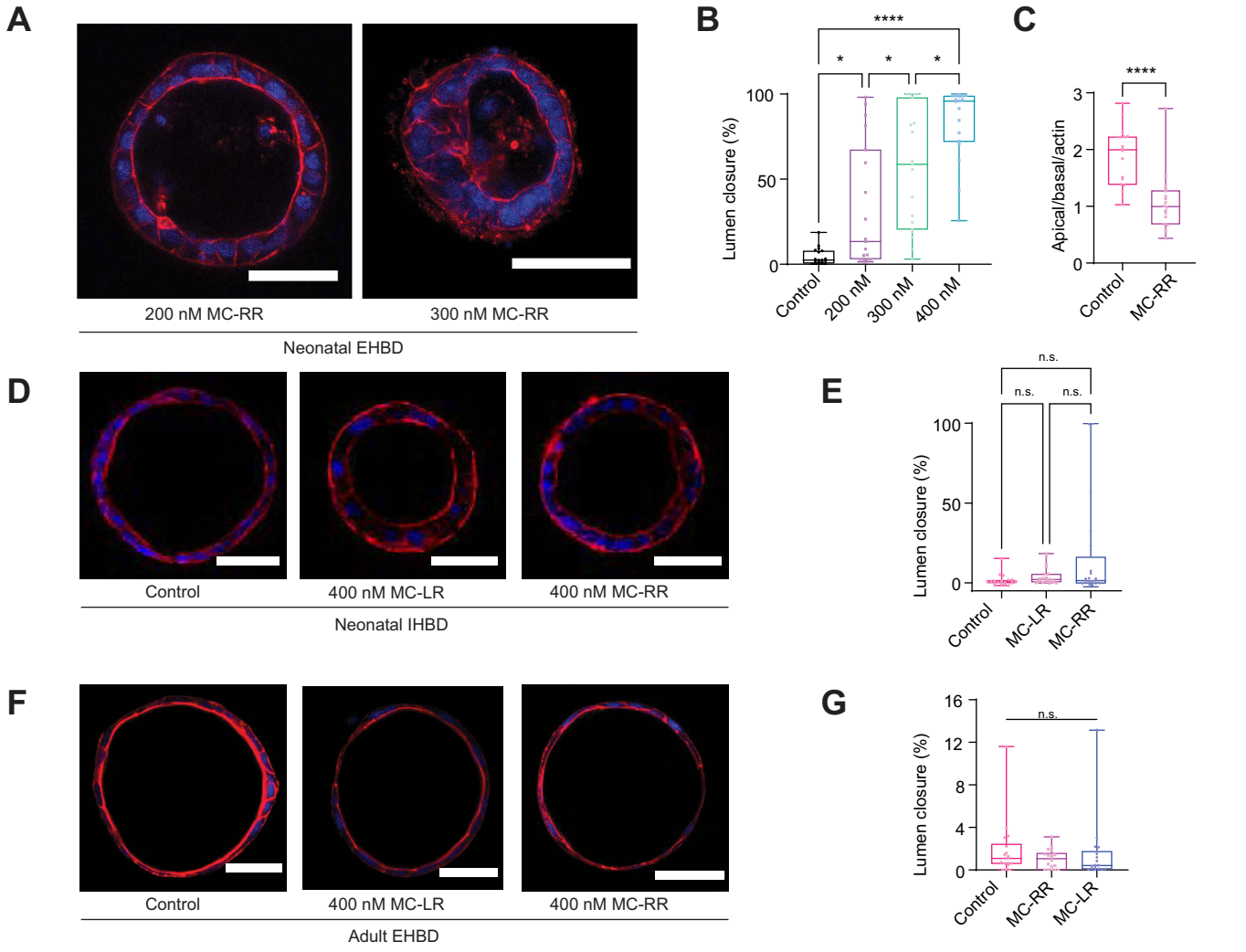

Fig. 2. Microcystin (MC)-RR-induced extrahepatic bile duct (EHBD) cholangiocyte spheroid collapse is specific for neonatal cholangiocytes. (A, B) MC-RR-induced neonatal EHBD cholangiocyte spheroid collapse at varying MC-RR concentrations. (A) Representative images of spheroids treated with 200 and 300 nM MC-RR. (B) Quantification showing dose dependence of lumen collapse. Data for 400 nM MC-RR are from the experiment reported in Fig. 1 in the main text: $p = 0.0125$, control *vs*. 200 nM MC-RR; $p < 0.0001$, control *vs*. 300 nM MC-RR; $p < 0.0001$, control *vs*. 400 nM MC-RR; $p = 0.0473$, 200 nM MC-RR *vs*. 300 nM MC-RR; $p < 0.0001$, 200 nM MC-RR *vs*. 400 nM MC-RR; $p = 0.0208$, 300 nM MC-RR *vs*. 400 nM MC-RR. (C) Quantification of loss of polarity (decrease in apical:basal actin ratio) in the presence of 400 nM MC-RR; $p < 0.0001$, determined using the unpaired two-tailed Student's *t* test. (D) Neonatal intrahepatic bile duct (IHBD) cholangiocyte spheroids show no damage after treatment with 400 nM of either MC-LR or MC-RR. (E) Quantification showing no difference in lumen closure after treatment of neonatal IHBD cholangiocytes with either MC-LR or MC-RR: $p = 0.8895$, control *vs*. MC-LR; $p = 0.0526$, control *vs*. MC-RR; $p = 0.1463$, MC-LR *vs*. MC-RR. (F) Adult EHBD cholangiocyte spheroids show no damage after treatment with 400 nM of either MC-LR or MC-RR. (G) Quantification showing no difference in lumen closure after treatment of adult EHBD cholangiocytes with either MC-LR or MC-RR: $p = 0.8821$, control *vs*. MC-LR; $p = 0.4366$, control *vs*. MC-RR; $p = 0.7288$, MC-LR *vs*. MC-RR. All images are representative of at least three independent experiments, with at least 18 spheroids quantified for lumen closure for each condition. Control spheroids are vehicle treated. Red indicates actin, blue indicates DAPI. Scale bars: 50 μm. Statistical significance in (B, E, G) determined using one-way ANOVA followed by multiple comparisons within each group and correction using Tukey's method, where: *$p \leq 0.05$, **$p \leq 0.01$, ***$p \leq 0.001$, and ****$p \leq 0.0001$.

MC-RR induces progressive and irreversible damage to neonatal EHBD cholangiocyte spheroids

The effect of 400 nM MC-RR on cholangiocyte spheroids was time dependent, with progressive damage observed over time, and significant damage was detected after 15 h of exposure (Fig. 3A and B). The damage was irreversible: removal of MC-RR-containing media and subsequent incubation with normal media did not result in recovery from lumen damage. Washout was tested at both early (15 h) and late (24 h) treatment times and no lumen recovery was found at either point (Fig. 3C; Fig. S5). However, spheroids treated for 15 h followed by washout (which had partial lumen closure) did not exhibit further lumen closure (Fig. 3C), indicating that persistent MC-RR exposure is necessary for progressive damage.

MC-RR causes damage to EHBDs in explant culture

Lumen closure, loss of monolayer integrity, and rounded cholangiocytes were observed when mouse P2 EHBD explants were cultured in a high oxygen incubator in the presence of 400 nM MC-RR (Fig. 4A and B). Using a qualitative scoring method (Fig. S3), these ducts were found to exhibit significantly higher damage compared with ducts cultured with either the

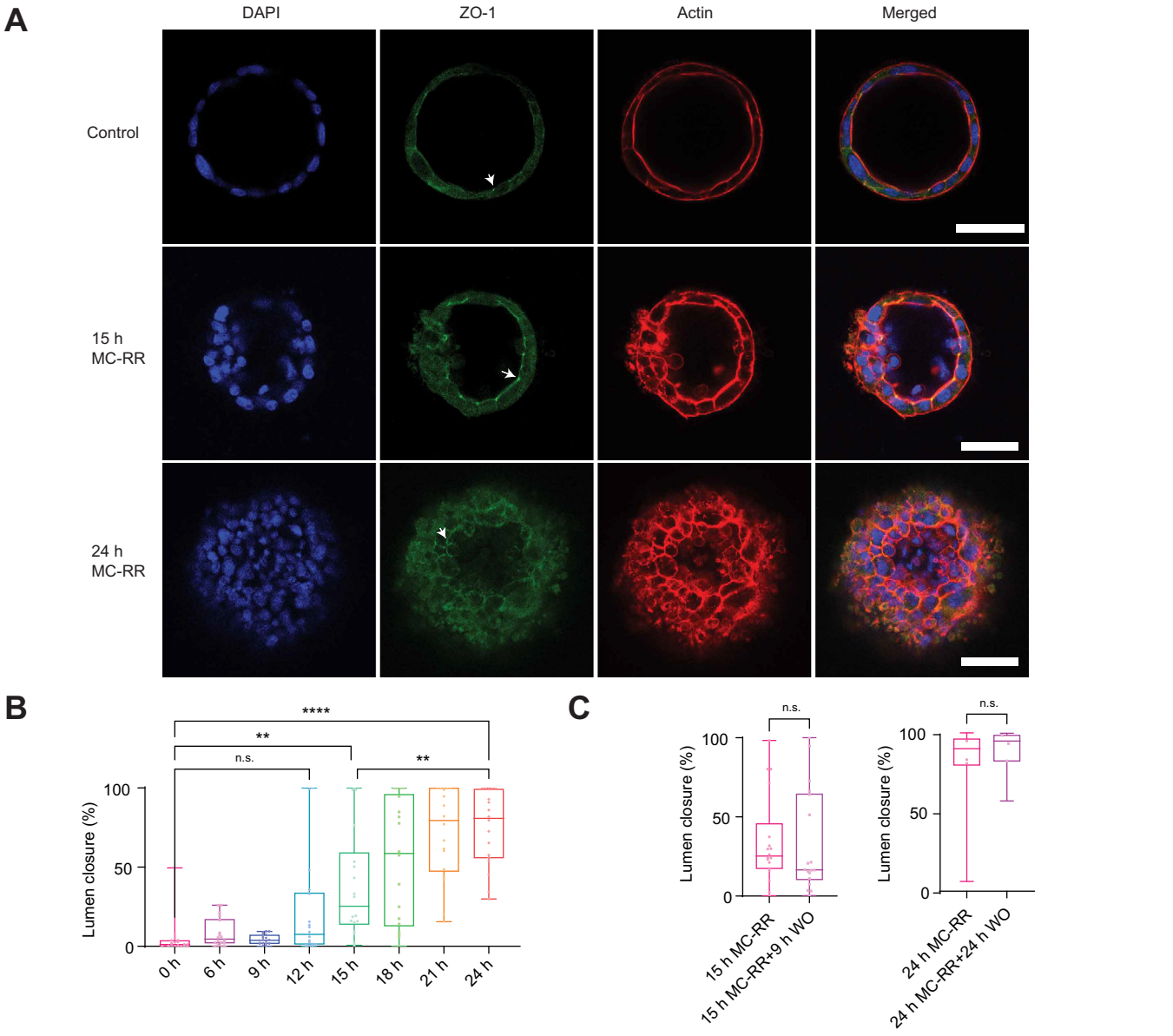

Fig. 3. Microcystin (MC)-RR induces progressive and irreversible spheroid lumen collapse. (A) Representative images of MC-RR (400 nm)-induced increasing neonatal extrahepatic bile duct (EHBD) cholangiocyte spheroid collapse with increasing treatment time. Cell–cell contacts, as marked by ZO-1 staining, were maintained (white arrowhead) as the damage progressed. (B) Quantification showing progressive lumen collapse with increasing MC-RR exposure time: $p = 0.5081$, 0 h *vs*. 12 h; $p = 0.003$, 0 h *vs*. 15 h; $p < 0.0001$, 0 h *vs*. 24 h; $p = 0.001$, 15 h *vs*. 24 h. Statistical significance determined using one-way ANOVA followed by multiple comparison within each group and correction using Tukey's method. (C) Quantification showing that MC-RR-induced damage was irreversible after 15 h or 24 h exposure and that lumen patency did not improve even after MC-RR washout (WO). Representative images shown in Fig. S5: $p = 0.8821$, 15 h MC-RR *vs*. 15 h MC-RR+ 9 h WO; $p = 0.2496$, 24 h MC-RR *vs*. 24 h MC-RR+ 24 h WO, determined using the unpaired two-tailed Student's *t* test. All images are representative of at least three independent experiments, with at least 18 spheroids quantified for lumen closure. Control spheroids are vehicle treated. Red indicates actin, green indicates ZO-1, blue indicates DAPI. Scale bars: 50 μm *$p \leq 0.05$, **$p \leq 0.01$, ***$p \leq 0.001$, and ****$p \leq 0.0001$.

vehicle control or 400 nM MC-LR (the most common and most studied microcystin, used hereafter as a control) (Fig. 4C). However, no damage was observed in EHBD explants from older (P15–18) mice cultured with either MC-LR or MC-RR (Fig. 5A and B). Rat EHBD explants showed similar results, with explants from P2 pups showing severe damage after treatment with 400 nM MC-RR (Fig. 5C and D; Fig. S6). These results show that MC-RR induces significant and neonate-selective damage to EHBD explants. This damage was associated with increased vimentin staining in both neonatal EHBD explants and cholangiocyte spheroids (Figs S7A–C and S8).

Mechanism of MC-RR-induced damage in neonatal cholangiocytes

Exposure to MC-RR did not cause apoptosis or proliferation of EHBD cholangiocytes, but instead resulted in the collapse of spheroids (Fig. 6A and B; Fig. S7D and E). In the control group, spheroids had an average diameter of 270 μm, suggesting ~220 cells per spheroid (assuming a spheroid thickness of 5 μm and a cell volume of 5,000 μm^3). In the 400 nM MC-RR treated group, the average spheroid diameter decreased to 127 μm, with a similar cell count of around 216 cells per

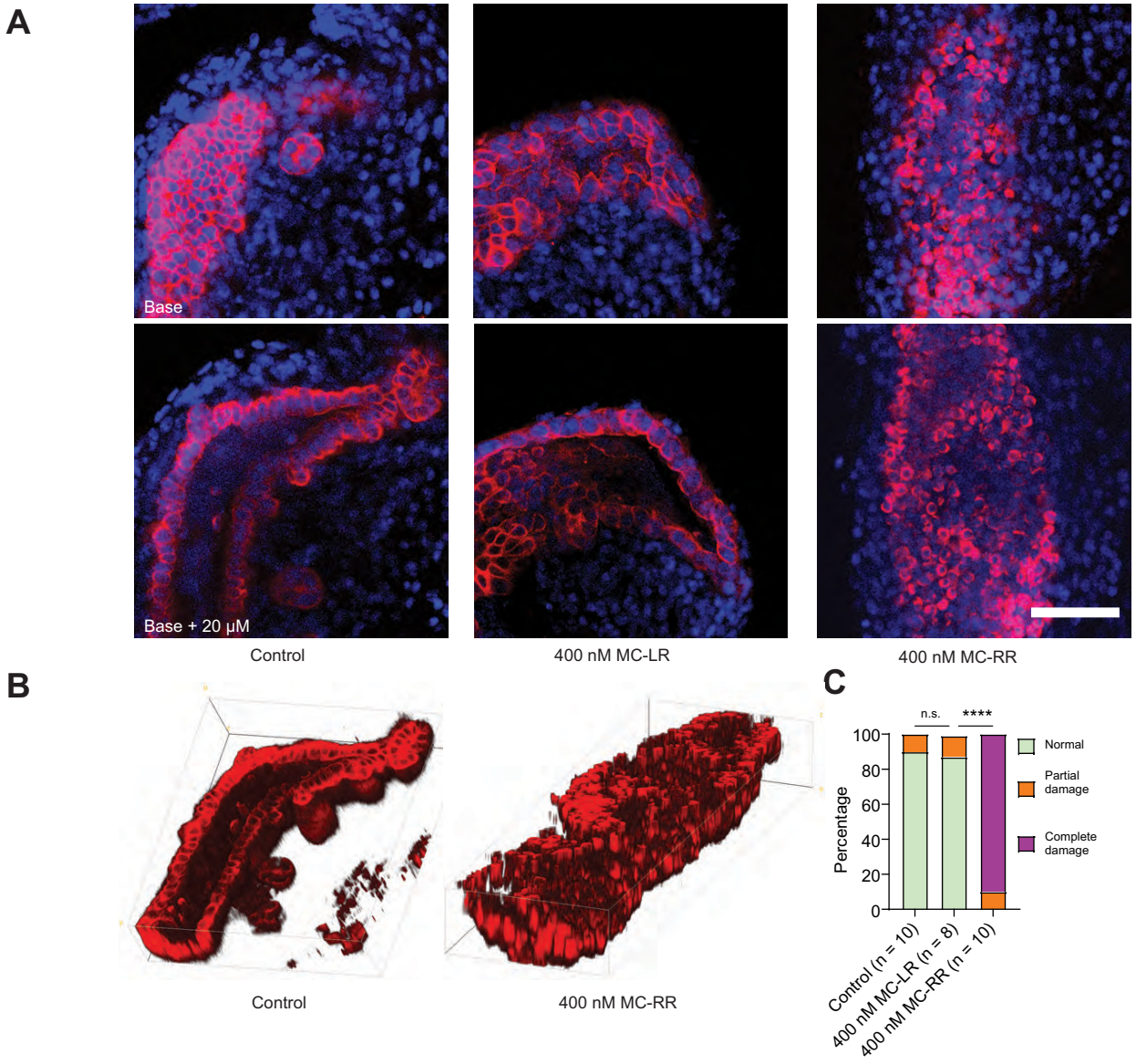

Fig. 4. Microcystin (MC)-RR treatment damages neonatal extrahepatic bile duct (EHBD) explants. (A) Representative image showing neonatal EHBD explants cultured in a high oxygen incubator in the presence of vehicle, 400 nM MC-LR, or 400 nM MC-RR for 24 h. EHBD explants were imaged using confocal microscopy; a base stack and a z-stack 20 μm above the base are shown. (B) 3D reconstruction of confocal images of EHBD explants treated with vehicle control and 400 nM MC-RR. (C) Quantification showing significant EHBD damage in the presence of 400 nM MC-RR (also see Fig. S3). The number of explants studied for each condition is given in parentheses. Each explant was derived from a different animal, with a total of 28 mouse pups used in the study: $p = 1.0$, control *vs*. MC-LR; $p < 0.0001$, control *vs*. MC-RR. Statistical significance determined using Fisher's exact test for count data. *$p \leq 0.05$, **$p \leq 0.01$, ***$p \leq 0.001$, and ****$p \leq 0.0001$. Red indicates KRT19, blue indicates DAPI. Scale bar: 50 μm.

spheroid (assuming complete collapse and a similar cell volume). This indicates that the observed effects are likely because of cells filling the spheroid rather than to cell proliferation, as the calculated cell number remained relatively constant despite the decrease in spheroid size.

In investigating the mechanism of MC-RR toxicity, we found that neonatal EHBD cholangiocytes took up significantly more MC-RR than MC-LR (Fig. 6C); however, uptake was similar for neonatal and adult cells (Fig. 6D), and in neonatal IHBD and EHBD cholangiocytes (Fig. 6C). The observed differences in neonatal MC-RR uptake were not a result of differential activity of members of the organic anion transport protein (OATP) family. Neonatal EHBDs preferentially express OATP2a1 with little to no detectable expression of other OATPs (OATP1a1, 1a4, 1a6, and 1b2) (Fig. 6E) and inhibiting OATP 2a1 using pranlukast or suramin[28] did not rescue cholangiocytes from MC-RR-induced damage (Fig. 6F; Fig. S9). Collectively, these data indicate that differential uptake of MC-RR is not the cause of neonatal cholangiocyte susceptibility to the toxin. Microcystin toxicity is often caused by inhibition of protein phosphatases, specifically (for MC-RR) phosphatase PP2A;[29] surprisingly, however, there was no reduction in PP2A activity in EHBD cholangiocytes in the presence of either 400 nM MC-RR or 400 nM MC-LR, suggesting a phosphatase-independent mechanism of cholangiocyte damage at this concentration (Fig. 6G and H).

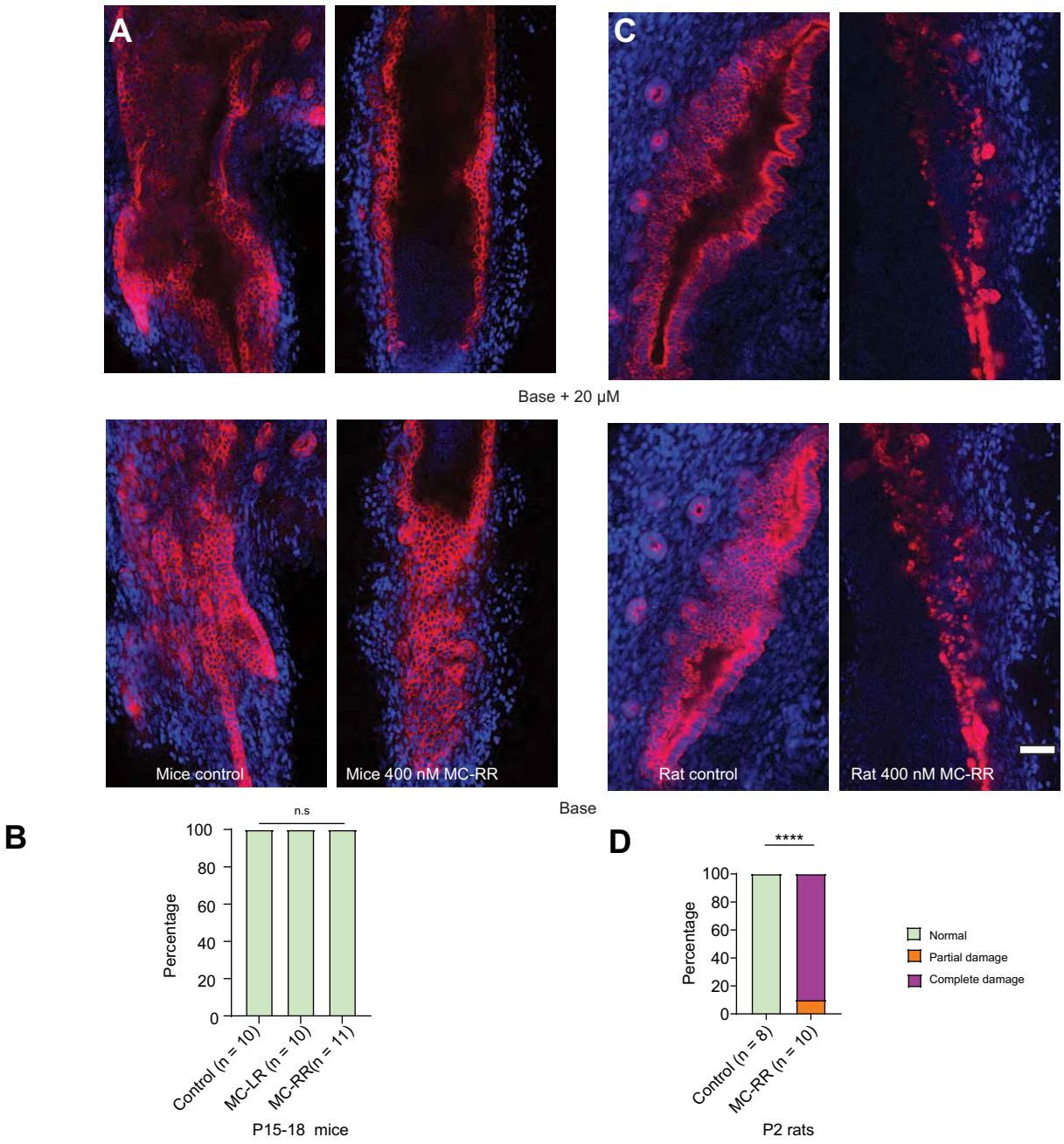

Fig. 5. Microcystin (MC)-RR does not damage extrahepatic bile duct (EHBD) after the neonatal period. (A) Representative images showing EHBDs isolated from postnatal day (P)15–18 mice cultured as explants in the presence of vehicle or 400 nM MC-RR. (B) Quantification showing lack of damage to EHBDs isolated from P15–18 mice pups: p =1.0, control *vs*. MC-LR; p = 1.0, control *vs*. MC-RR. (C) Representative image showing EHBDs isolated from P2 rat pups cultured as explants in the presence of vehicle or 400 nM MC-RR. (D) Quantification showing damage to EHBDs isolated from P2 rat pups: p <0.0001, control *vs*. MC-RR. The number of explants studied per condition is shown in parentheses. Each explant was derived from a different animal. (B) shows data from a total of 31 P15–18 mice pups, whereas (D) shows data from a total of 18 P2 rat pups. Red indicates KRT19, blue indicates DAPI. Scale bar: 50 μm. Statistical significance in (B, D) determined using Fisher's exact test for count data: *p ≤0.05, **p ≤0.01, ***p ≤0.001, and ****p ≤0.0001.

We then considered the role of redox stress in MC-RR-induced cholangiocyte toxicity, given that it may be a common mechanism of EHBD toxicity.[14,19,30] Treatment with MC-RR induced higher levels of reactive oxygen species (ROS) in neonatal EHBD cholangiocyte spheroids compared with MC-LR (Fig. 7A). In additional, ROS levels in MC-RR-treated neonatal cholangiocytes were markedly higher than for adult EHBD cholangiocyte spheroids treated with either MC-LR or MC-RR (Fig. 7B; Fig. S10). Neonatal (compared with adult) mouse EHBDs exhibit reduced levels of glutathione (Fig. 7C) and various redox enzymes, including glutathione peroxidase (GPX)-1, GPX-4, catalase (CAT), and superoxide dismutase (SOD)-1 (Fig. 7D), suggesting a differential susceptibility to redox stress in neonatal

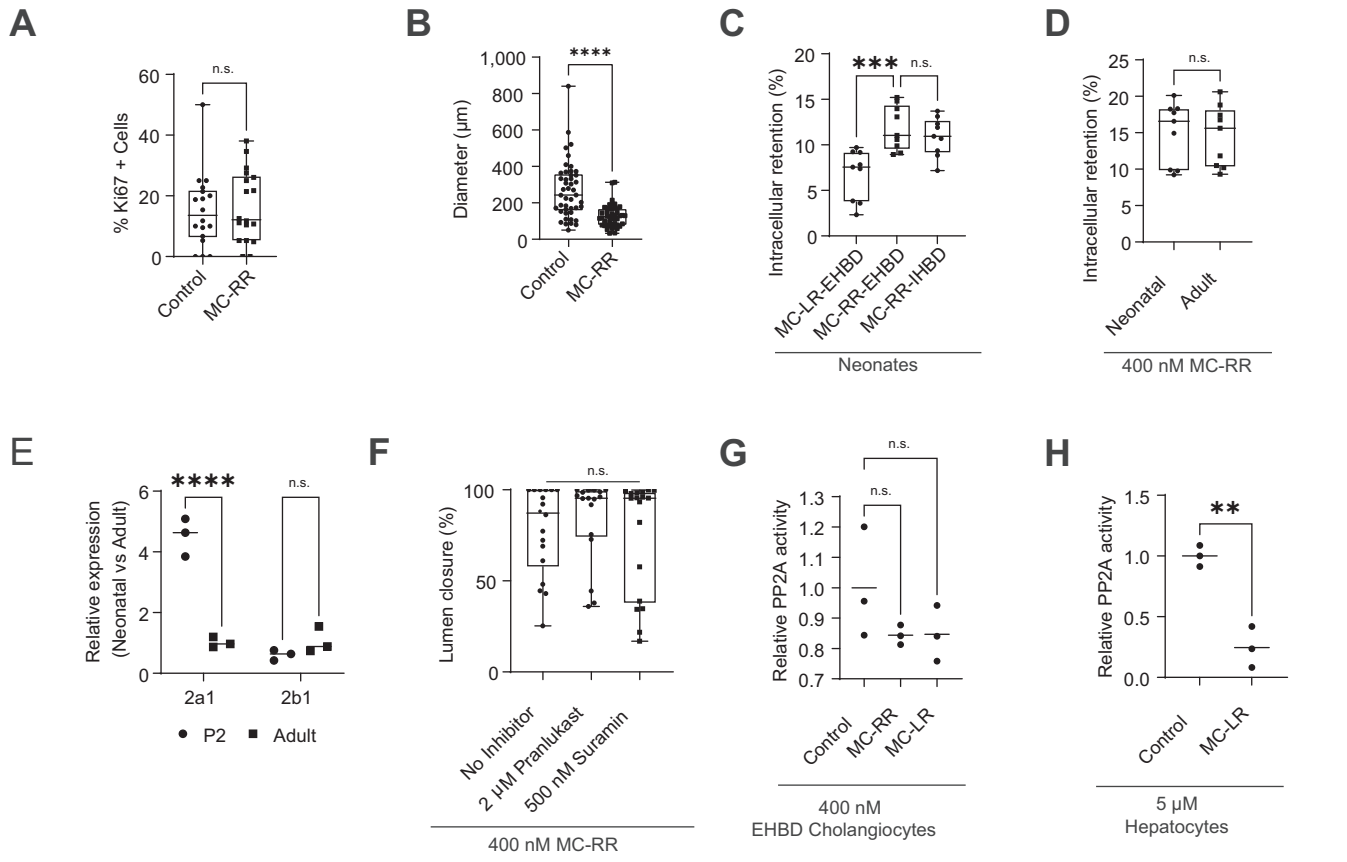

Fig. 6. Mechanism of microcystin (MC)-RR-induced injury. (A) Quantification of Ki67+ cells in neonatal mouse extrahepatic bile duct (EHBD) cholangiocyte spheroids treated with vehicle or 400 nM MC-RR (n = 18 per condition from three independent experiments): $p = 0.7298$, determined using the unpaired two-tailed Student's *t* test. (B) Spheroid diameter after treatment with vehicle or 400 nM MC-RR (n = 45 spheroids per condition from three independent experiments): $p < 0.0001$, determined using the unpaired two-tailed Student's *t* test. (C) Relative retention of MC-LR and MC-RR in neonatal EHBD cholangiocytes and MC-RR in neonatal intrahepatic bile duct (IHBD) cholangiocytes (n = 9 samples from three independent experiments): $p = 0.0005$, MC-LR EHBD *vs*. MC-RR EHBD; $p = 0.6945$, MC-RR EHBD *vs*. MC-RR IHBD. Statistical significance determined using one-way ANOVA followed by multiple comparison within each group and correction using Tukey's method. (D) MC-RR retention in neonatal and adult EHBD cholangiocytes (n = 9 samples from each condition across three independent experiments): $p = 0.8367$, determined using the unpaired two-tailed Student's *t* test. (E) Relative mRNA expression of organic anion transport protein (OATP)-2a1 and 2b1 in neonatal EHBD compared with adult EHBD. OATP1a1, 1a4, 1a6, and 1b2 were below the detection limit in neonatal samples (three independent experiments): $p < 0.0001$, P2 *vs*. adult for 2a1 and $p = 0.3731$for 2b1. Statistical significance determined using two-way ANOVA followed by multiple comparison using Sidak's multiple comparison test. (F) Quantification showing no significant difference in MC-RR-induced lumen damage with simultaneous OATP2a1 inhibition using suramin and pranlukast (n = 18 spheroids per condition from three independent experiments): $p = 0.7559$, no inhibitor *vs*. 2 μM pranlukast: $p = 0.9530$, no inhibitor *vs*. 500 nM suramin. Statistical significance determined using one-way ANOVA followed by multiple comparison within each group and correction using Tukey's method. (G) Relative PP2A activity in neonatal EHBD cholangiocytes treated with vehicle, 400 nM MC-LR, or 400 nM MC-RR: $p = 0.3265$, control *vs*. MC-LR; $p = 0.3159$, control *vs*. MC-RR. Statistical significance determined using one-way ANOVA followed by multiple comparison within each group and correction using Tukey's method. (H) Control experiments showing decreased relative PP2A activity in hepatocytes treated with 5 μM MC-LR: $p < 0.0023$, determined using unpaired two-tailed Student's *t* test. *$p \leq 0.05$, **$p \leq 0.01$, ***$p \leq 0.001$, and ****$p \leq 0.0001$.

cholangiocytes,[13,19,31] which explains why they, unlike adult cholangiocytes, are sensitive to MC-RR.

N-acetyl cysteine rescues MC-RR-induced damage

To further evaluate the role of redox in MC-RR-induced EHBD cholangiocyte damage, GSH levels were measured in neonatal EHBD cholangiocytes in the presence and absence of MC-RR. Treatment of neonatal EHBDs, but not IHBDs, with MC-RR led to significant depletion of GSH levels (Fig. 8A; Fig. S11). Given the role of GSH, it was hypothesized that treating neonatal EHBD cholangiocyte spheroids with NAC would protect against damage from MC-RR. Cholangiocytes treated with 300 nM MC-RR and NAC were not significantly different from the control group ($p = 0.06$), whereas those treated with 300 nM MC-RR alone were significantly different from the control ($p < 0.05$). Nevertheless, the GSH levels in cholangiocytes treated with either MC-RR or MC-RR and NAC were similar (Fig 8A). Therefore, it was concluded that NAC did not offer any significant advantage in replenishing GSH levels in the presence of MC-RR. In addition, treatment with NAC during exposure to 300 nM MC-RR resulted in blunting but not prevention of the phenotype, with obvious cholangiocyte damage but maintenance of the hollow lumen and preservation of monolayer integrity (Fig. 8B). However, spheroids treated with 400 nM MC-RR showed no protection from damage if simultaneously treated with NAC, suggesting that the higher concentration of MC-RR overwhelmed the protective effects of NAC (Fig. 8C; Fig. S12). Similarly, in P2 mouse EHBD explant cultures, treatment with NAC coincident with 300 mM MC-RR led to

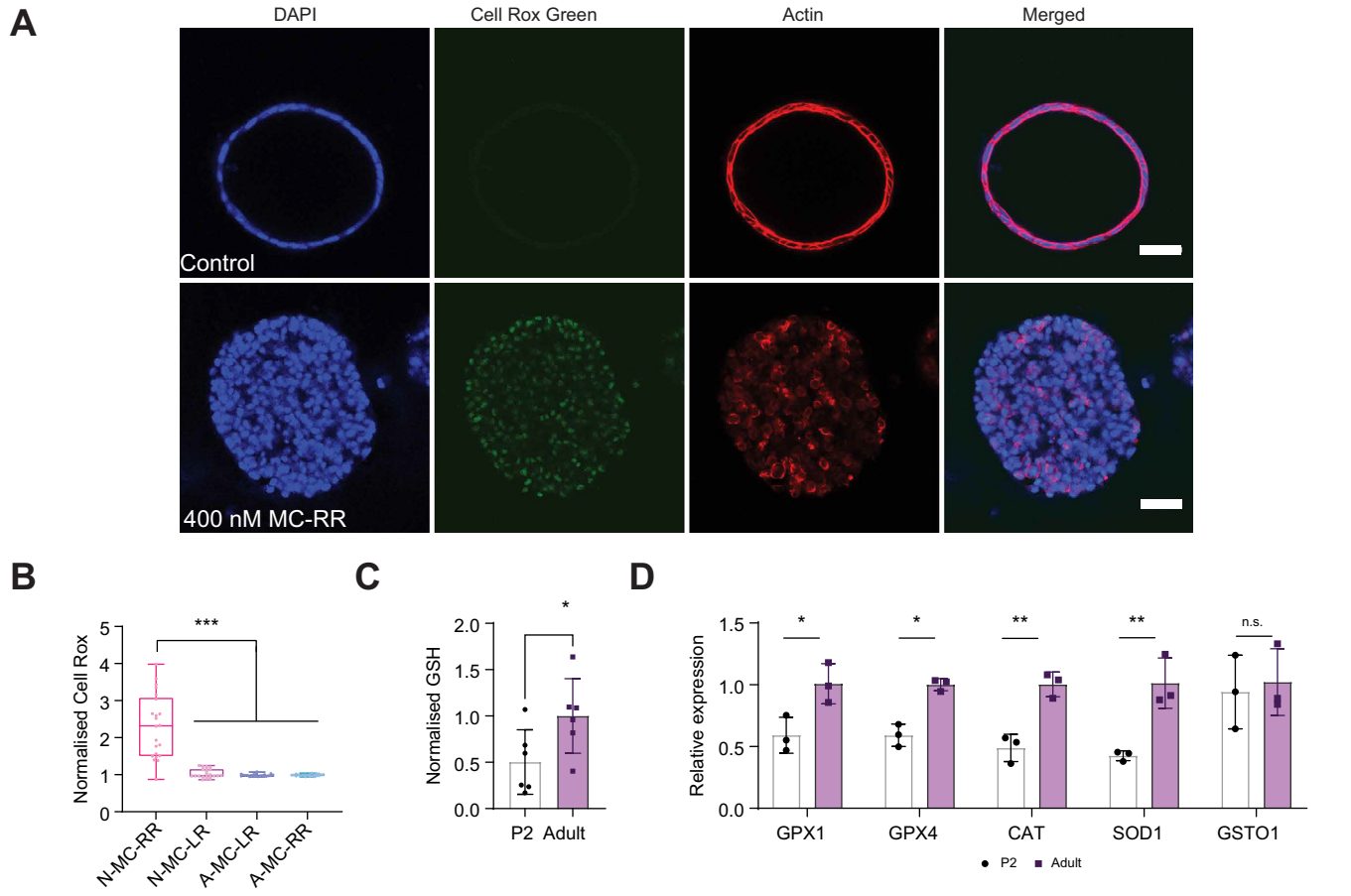

Fig. 7. Microcystin (MC)-RR induces elevated reactive oxygen species (ROS) in neonatal extrahepatic bile duct (EHBD) cholangiocyte spheroids. (A) ROS production in the presence of vehicle or 400 nM MC-RR. Images are representative of three independent experiments with at least 18 spheroids quantified for lumen closure per condition. Red indicates actin, green indicates Cell-Rox Green, blue indicates DAPI. Scale bars: 50 μm. (B) Quantification of ROS production in neonatal and adult EHBD cholangiocyte spheroids after treatment with 400 nM MC-LR or 400 nM MC-RR for 24 h: p <0.0001 for N-MC-RR *vs*. N-MC-LR, A-MC-RR, and A-MC-LR. Statistical significance determined using one-way ANOVA followed by multiple comparison within each group and correction using Tukey's method. (C) GSH levels were quantified in protein samples obtained from EHBDS of P2 and adult mice, showing significantly lower GSH levels in neonates compared with adults (n = 6 ducts each condition): p <0.045, determined using unpaired two-tailed Student's t test. (D) RNA samples from the EHBDs of P2 and adult mice were assayed by real-time PCR for enzymes involved in antioxidant defense systems. The data, which are normalized to expression levels in adult samples, demonstrate that all measured enzymes except GSTO-1 were significantly lower in neonatal compared with adult ducts (n = 3 EHBDs each, two technical replicates per sample): p = 0.033, P2 *vs.* adult for GPX1; p = 0.0372, P2 *vs.* adult for GPX4; p = 0.0066, P2 *vs.* adult for CAT; p = 0.0019, P2 *vs.* adult for SOD1; p = 0.9848, P2 *vs.* adult for GSTO1. Statistical significance determined using two-way ANOVA followed by multiple comparison using Sidak's multiple comparison test. Error bars denote standard deviation. *p ≤0.05, **p ≤0.01, ***p ≤0.001, and ****p ≤0.0001.

partial amelioration of the phenotype compared with 300 nM MC-RR treatment, but no difference was observed with or without NAC when explants were treated with 400 nM MC-RR (Fig. 8D and E; Fig. S8).

Discussion

Neonatal cholestatic diseases, including BA, are a major cause of pediatric liver diseases and pose significant treatment challenges.[7] Although the cause of most cases of BA is unknown, recent research provides a proof of concept in animal models that toxin exposure can cause a BA-like syndrome in neonates.[14,16,17] Toxins potentially responsible for BA in humans have not been identified, and the toxin responsible for BA in neonatal livestock, biliatresone, is an unlikely source of exposure for humans.[9] In this work, we examined the microcystins, a family of widely distributed toxins with significance to humans that, similar to biliatresone, are electrophilic carbonyl compounds.[18,32] We showed that one microcystin of seven tested, MC-RR, was toxic to rodent cholangiocytes and EHBD explants. Notably, this toxicity was selective for neonatal, but not adult EHBDs. MC-RR specifically caused significant elevations in ROS in neonatal cholangiocytes and EHBD explants, suggesting this as its likely mechanism of action.

Microcystins are produced by cyanobacteria (blue-green algae), mainly *Microcystis* species, during harmful algal blooms.[24] They are found globally and cause significant harm to both humans and wildlife,[23,33] an impact that is predicted to increase with climate change. The maximum safe value for MC-LR in drinking water, as established by the World Health Organization, is 1 μg/L (~1 nM).[34] There are no specific guidelines for other microcystins and their toxicity is less well understood,[34,35] but, of note, we were unable to locate reports of bile duct toxicity related to any of the microcystins.

MC-RR did not cause apoptosis or cell death, as determined by TUNEL staining and an MTT assay, but instead

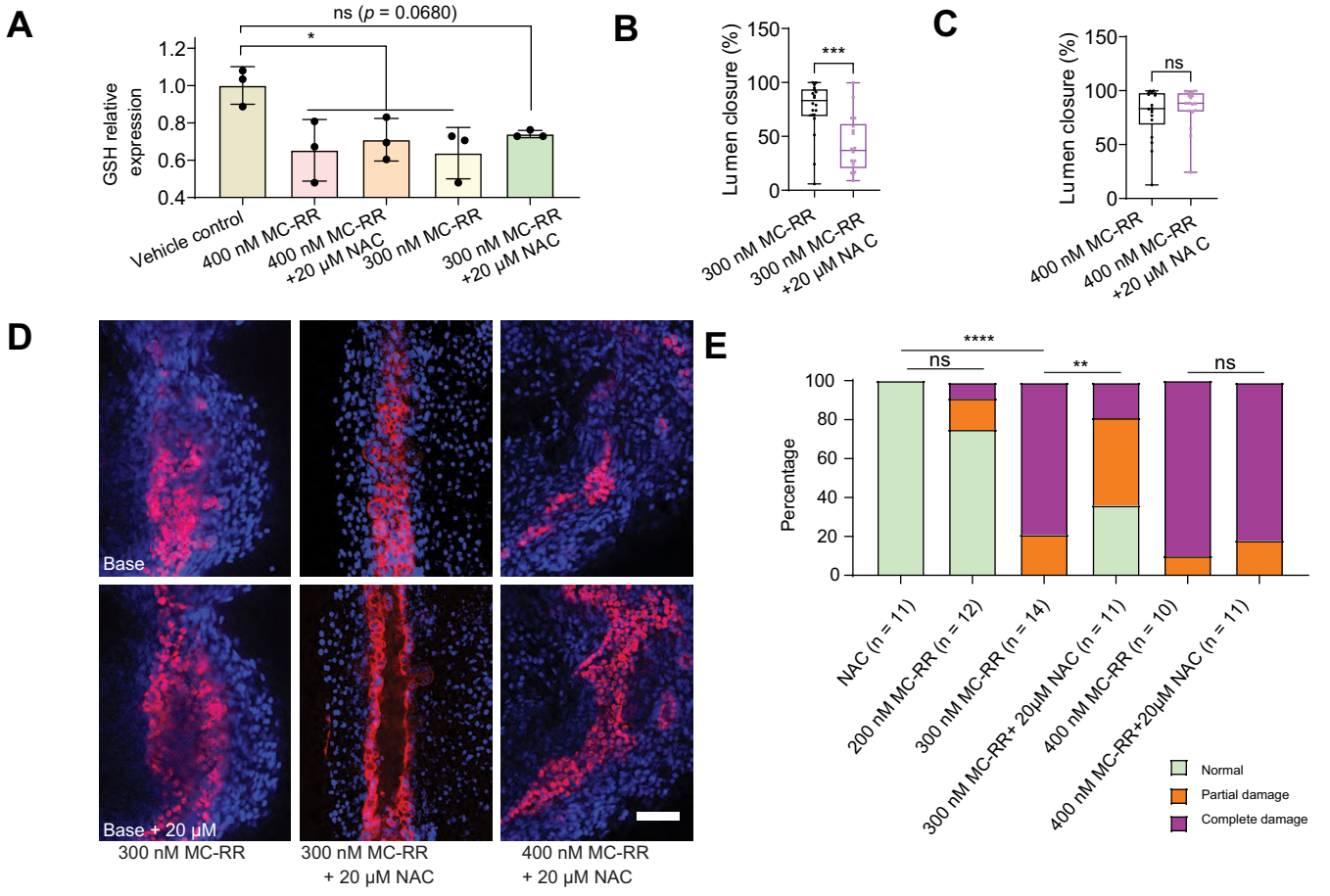

Fig. 8. *N*-acetyl cysteine (NAC) partially ameliorates MC-RR induced damage in spheroids and extrahepatic bile ducts (EHBDs). (A) Relative glutathione (GSH) level in EHBD cholangiocytes treated with 300 nM and 400 nM MC-RR as well as MC-RR along with 20 μM NAC (n = 3): $p = 0.0157$, vehicle control *vs*. 400 nM MC-RR; $p = 0.0408$, vehicle control *vs*. 400 nM MC-RR + 20 μM NAC; $p = 0.0122$, vehicle control *vs*. 300 nM MC-RR; $p = 0.0680$, vehicle control *vs*. 300 nM MC-RR + 20 μM NAC. Statistical significance determined using one-way ANOVA followed by multiple comparison with vehicle control and correction using Dunnett's method. (B) Lumen closure in neonatal EHBD cholangiocyte spheroids treated with 300 nM MC-RR ± NAC for 24 h: $p < 0.0004$, determined using unpaired two-tailed Student's *t* test. (C) Lumen closure in neonatal EHBD cholangiocyte spheroids treated with 400 nM MC-RR ± NAC: $p = 0.4226$, determined using unpaired two-tailed Student's *t* test. (D) Representative images showing MC-RR-induced EHBD damage at different MC-RR concentrations and in the presence of NAC. (E) Quantification of EHBD explant damage after treatment with increasing MC-RR concentrations with and without NAC. Numbers of explants examined per condition are in parentheses. Each explant was derived from a different animal. Data from a total of 69 pups: $p = 0.3416$, NAC *vs*. 200 nM MC-RR; $p < 0.0001$, NAC *vs*. 300 nM MC-RR; $p = 0.0043$, 300 nM MC-RR *vs*. 300 nM MC-RR + 20 μM NAC; $p = 1.0$, 400 nM MC-RR *vs*. 400 nM MC-RR + 20 μM NAC. Statistical significance determined using Fisher's exact test for count data. Red indicates KRT19, blue indicates DAPI. Scale bar: 50 μm $^{*}p \leq 0.05$, $^{**}p \leq 0.01$, $^{***}p \leq 0.001$, and $^{****}p \leq 0.0001$.

resulted irreversibly in a loss of apical–basal polarity and architectural re-organization of the cholangiocyte monolayer in spheroids and EHBD explants. Increases in vimentin staining suggested a partial epithelial-to-mesenchymal transition (EMT),[36] potentially aiding the cell migration or extrusion into the lumen that ultimately led to lumen obstruction. The EMT appeared to be at least partially independent of ROS, because vimentin expression also occurred in cholangiocytes following NAC treatment.

The specificity of MC-RR for neonatal, as opposed to adult, EHBD cholangiocytes and EHBDs was striking, particularly because MC-LR, which is more hepatotoxic than MC-RR,[21] had no demonstrable effects. Treatment of cholangiocytes with MC-RR resulted in higher intracellular levels compared with treatment with MC-LR, although this was true for both neonatal and adult cells, and, thus, did not explain neonatal-specific toxicity. Similarly, IHBD and EHBD cholangiocytes accumulated MC-RR to equivalent extents, although only EHBD cholangiocyte were sensitive to MC-RR. Although microcystin uptake is often linked to OATPs, the literature does not provide a clear understanding of the specific OATP involved in MC-RR uptake in mice. Of all the OATPs examined, the only OATP found to be expressed on neonatal EHBDs was OATP2a1, a prostaglandin transporter[37] with an unknown role in microcystin uptake. Treatment of spheroids with the known OATP2a1 inhibitors pranlukast and suramin[28] had no effect on uptake, suggesting that MC-RR enters cholangiocytes independent of OATP2a1. Microcystins target various organs, such as intestine, liver, and kidney, in mammals and, although they are mainly taken up in liver via OATPs, it is still not known how they are internalized by other organs. such as kidney.[23] Many cell lines (including liver stem cell lines) that lack OATPs are also known to take up microcystins,[38] suggesting that there are other (currently unknown) transporters or cellular uptake mechanisms for microcystins.

The R^1-position arginine of MC-RR appears to be necessary for toxicity, because neither MC-LR nor MC-YR had any effect on cholangiocytes. Unfortunately, we were unable to test whether the R^1 arginine was sufficient for toxicity. Although the

existence of MC-RX compounds has been reported, none are available commercially and most have been identified only by liquid chromatography–mass spectrometry (LC-MS);[32] we were unable to locate any in sufficient amounts even through private sources. The presence of two arginine residues in MC-RR likely alters the microcystin ring structure, and understanding the role of these dibasic residues may be key to understanding MC-RR toxicity. Arginine residues in peptides can promote cellular uptake via direct translocation and endocytotic pathways;[39] however, whether the presence of two arginines in MC-RR promotes cellular uptake via this mechanism is not known.

The extrahepatic biliary system of neonates has lower levels of GSH compared with the intrahepatic system or adult ducts in either location, and has lower levels of key antioxidant pathway enzymes. This appears to have a key role in biliatresone toxicity.[13,19,31] Our finding that MC-RR was specific for neonatal EHBD cholangiocytes and induced higher levels of ROS in the neonatal EHBD is consistent with lower levels of GSH in the EHBD and with a role for oxidative stress in the mechanism of action of MC-RR. MC-RR treatment further depleted the GSH pool in EHBD cholangiocytes, further suggesting involvement of oxidative stress in MC-RR induced damage. Recently reported research based on RNA sequencing of samples obtained during Kasai hepatoportoenterostomy surgery for BA suggests that a ROS-related mechanism has a role in BA: oxidative pathways were found to be disturbed in a significant fraction of patients with BA.[40] The effects of NAC, which replenishes cellular GSH and also directly interacts with, and neutralizes ROS, including superoxide anions and hydroxyl radicals, suggest that it could be used as a preventive or therapeutic agent[41] and, indeed, there is an ongoing clinical trial testing whether NAC has efficacy in BA.[42] However, given that NAC only partially prevented MC-RR-induced damage in our rodent model systems, mechanisms in addition to redox stress might be involved.

We investigated microcystins because of their structural similarity to biliatresone. Although there were similarities in the effects of the two toxins on neonatal cholangiocytes, there were also notable differences. Biliatresone-induced damage required continuous exposure to the compound, with spheroids recovering after the removal of biliatresone (at least within a certain time frame[15]), whereas MC-RR-treated spheroids did not show recovery after drug washout. The presence of an unsaturated carbonyl group in and of itself does not necessarily render a compound toxic. This is evident from the fact that other microcystins, which also contain this group, have no visible effect on cholangiocytes. These findings suggest that the mechanism underlying toxin-induced cholangiocyte damage is complex and warrants further investigation.

The frequency of harmful algal blooms is projected to increase as climate change progresses.[43] Human exposure to microcystins will likely increase in parallel. In the USA, the incidence of BA has shown an upward trend, increasing from 28.5 cases per million births in 1997 to 55.5 cases per million births in 2012.[44] Although the appearance of BA does not exhibit clear seasonal patterns,[45,46] there have been certain periods during which an increase in BA has been observed.[47–51] To determine whether there is a connection between maternal exposure to MC-RR and the development of BA, further mechanistic studies and epidemiological investigations are needed. Although MC-LR has been extensively studied, exploring the potential relationship between microcystins and BA will require more detailed studies of MC-RR, as opposed to MC-LR, in both bodies of water and the food chain.

Affiliations

[1]*Division of Gastroenterology and Hepatology, Department of Medicine, University of Pennsylvania, Philadelphia, PA, USA;* [2]*Center for Engineering MechanoBiology, University of Pennsylvania, Philadelphia, PA, USA;* [3]*Department of Bioengineering, University of Pennsylvania, Philadelphia, PA, USA*

Abbreviations

BA, biliary atresia; BEC, biliary epithelial cell; CAT, catalase; EHBD, extrahepatic bile duct; GSH, glutathione; GPX-1, glutathione peroxidase; IACUC, Institutional Animal Care and Use Committee; IHBD, intrahepatic bile duct; LC-MS, liquid chromatography–mass spectrometry; MC-LR, Microcystin-LR; MC-RR, microcystin-RR; NAC, N-acetyl cysteine; OATP, organic anion transport protein; ROS, reactive oxygen species; SOD-1, superoxide dismutase 1.

Financial support

This study was supported by a pilot grant from the UPenn/NIEHS Center of Excellence in Environmental Toxicology (P30 ES013508), by NIH R01 DK119290, and by the Fred and Suzanne Biesecker Pediatric Liver Center at The Children's Hospital of Philadelphia, all to RGW.

Conflicts of interest

The authors declare no conflict of interest.

Please refer to the accompanying ICMJE disclosure forms for further details.

Authors' contributions

Conceptualization: KG, RGW. Formal analysis: KG. Methodology: KG, DC. Investigation: KG. Writing - original draft: KG. Resources, funding acquisition, supervision, writing - review and editing: RGW.

Data availability statement

The data that support the findings of this study are available from the corresponding author upon reasonable request.

Acknowledgements

We are grateful to the UPenn Cell and Developmental Biology Microscopy Core and the NIDDK Center for Molecular Studies in Digestive and Liver Diseases Molecular Pathology and Imaging Core (P30 DK050306) for technical support.

Supplementary data

Supplementary data to this article can be found online at https://doi.org/10.1016/j.jhepr.2024.101218.

References

Author names in bold designate shared first authorship

[1] Vic P, Gestas P, Mallet E, et al. L'atrésie des voies biliaires en polynésie française. Étude rétrospective sur 10 ans. Arch Pediatr 1994;1:646–651.

[2] Tiao MM, Tsai SS, Kuo HW, et al. Epidemiological features of biliary atresia in Taiwan, a national study 1996-2003. J Gastroenterol Hepatol 2008;23:62–66.

[3] Mack CL. What causes biliary atresia? Unique aspects of the neonatal immune system provide clues to disease pathogenesis. Cell Mol Gastroenterol Hepatol 2015;1:267–274.

[4] de Jong IEM, Hunt ML, Chen D, et al. A fetal wound healing program after intrauterine bile duct injury may contribute to biliary atresia. J Hepatol 2023;79:1396–1407.

[5] Quelhas P, Cerski C, dos Santos JL. Update on etiology and pathogenesis of biliary atresia. Curr Pediatr Rev 2022;19:48–67.

[6] Harpavat S, Garcia-Prats JA, Anaya C, et al. Diagnostic yield of newborn screening for biliary atresia using direct or conjugated bilirubin measurements. JAMA 2020;323:1141–1150.

[7] Schreiber RA, Harpavat S, Hulscher JBF, et al. Biliary atresia in 2021: epidemiology, screening and public policy. J Clin Med 2022;11:999.
[8] Harper P, Plant JW, Unger DB. Congenital biliary atresia and jaundice in lambs and calves. Aust Vet J 1990;67:18–22.
[9] **Lorent K**, **Gong W**, **Koo KA**, et al. Identification of a plant isoflavonoid that causes biliary atresia. Sci Transl Med 2015;7:286ra67.
[10] Lakshminarayanan B, Davenport M. Biliary atresia: a comprehensive review. J Autoimmun 2016;73:1–9.
[11] Davenport M, Ong E, Sharif K, et al. Biliary atresia in England and Wales: results of centralization and new benchmark. J Pediatr Surg 2011;46:1689–1694.
[12] **Zani A**, **Quaglia A**, Hadzić N, et al. Cytomegalovirus-associated biliary atresia: an aetiological and prognostic subgroup. J Pediatr Surg 2015;50:1739–1745.
[13] Fried S, Gilboa D, Har-Zahav A, et al. Extrahepatic cholangiocyte obstruction is mediated by decreased glutathione, Wnt and Notch signaling pathways in a toxic model of biliary atresia. Sci Rep 2020;10:7599.
[14] Yang Y, Wang J, Zhan Y, et al. The synthetic toxin biliatresone causes biliary atresia in mice. Lab Investig 2020;100:1425–1435.
[15] Waisbourd-Zinman O, Koh H, Tsai S, et al. The toxin biliatresone causes mouse extrahepatic cholangiocyte damage and fibrosis through decreased glutathione and SOX17. Hepatology 2016;64:880–893.
[16] Gupta K, Xu JP, Diamond T, et al. Biliatresone treatment of pregnant mice causes changes in bile metabolism and liver inflammation in their offspring. BioRxiv 2023;19:e0301824. https://doi.org/10.1101/2023.03.02.530913. Published online March 3.
[17] Schmidt H, Hagens J, Schuppert P, et al. Biliatresone and biliary atresia -disease modelling in C57BL/6J neonates. Sci Rep 2023;13:10574.
[18] Estrada MA, Zhao X, Lorent K, et al. Synthesis and structure-activity relationship study of biliatresone, a plant isoflavonoid that causes biliary atresia. ACS Med Chem Lett 2018;9:61–64.
[19] Zhao X, Lorent K, Wilkins BJ, et al. Glutathione antioxidant pathway activity and reserve determine toxicity and specificity of the biliary toxin biliatresone in zebrafish. Hepatology 2016;64:894–907.
[20] Buratti FM, Manganelli M, Vichi S, et al. Cyanotoxins: producing organisms, occurrence, toxicity, mechanism of action and human health toxicological risk evaluation. Arch Toxicol 2017;91:1049–1130.
[21] Srivastava A, Choi GG, Ahn CY, et al. Dynamics of microcystin production and quantification of potentially toxigenic *Microcystis* sp. using real-time PCR. Water Res 2012;46:817–827.
[22] Bouhaddada R, Nélieu S, Nasri H, et al. High diversity of microcystins in a *Microcystis* bloom from an Algerian lake. Environ Pollut 2016;216:836–844.
[23] Arman T, Clarke JD. Microcystin toxicokinetics, molecular toxicology, and pathophysiology in preclinical rodent models and humans. Toxins (Basel) 2021;13:537.
[24] Melaram R, Newton AR, Chafin J. Microcystin contamination and toxicity: implications for agriculture and public health. Toxins (Basel) 2022;14:350.
[25] Mutoti MI, Edokpayi JN, Mutileni N, et al. Cyanotoxins in groundwater; occurrence, potential sources, health impacts and knowledge gap for public health. Toxicon 2023;226:107077.
[26] Karjoo S, Wells RG. Isolation of neonatal extrahepatic cholangiocytes. J Vis Exp 2014;88:51621.
[27] **Dipaola F**, **Shivakumar P**, Pfister J, et al. Identification of intramural epithelial networks linked to peribiliary glands that express progenitor cell markers and proliferate after injury in mice. Hepatology 2013;58:1486–1496.
[28] Kamo S, Nakanishi T, Aotani R, et al. Impact of FDA-approved drugs on the prostaglandin transporter OATP2A1/SLCO2A1. J Pharm Sci 2017;106:2483–2490.
[29] Ikehara T, Imamura S, Sano T, et al. The effect of structural variation in 21 microcystins on their inhibition of PP2A and the effect of replacing cys269 with glycine. Toxicon 2009;54:539–544.
[30] Salunga TL, Cui Z-G, Shimoda S, et al. Oxidative stress-induced apoptosis of bile duct cells in primary biliary cirrhosis. J Autoimmun 2007;29:78–86.
[31] Zhao X, Lorent K, Escobar-Zarate D, et al. Impaired redox and protein homeostasis as risk factors and therapeutic targets in toxin-induced biliary atresia. Gastroenterology 2020;159:1068–1084.
[32] Bouaïcha N, Miles CO, Beach DG, et al. Structural diversity, characterization and toxicology of microcystins. Toxins (Basel) 2019;11:714.
[33] Rattner BA, Wazniak CE, Lankton JS, et al. Review of harmful algal bloom effects on birds with implications for avian wildlife in the Chesapeake Bay region. Harmful Algae 2022;120:102319.
[34] WHO. *Cyanobacterial Toxins*. Microcystins. Background document for development of WHO guidelines for drinking-water quality and guidelines for safe recreational water environments. Geneva: WHO; 2020.
[35] Díez-Quijada L, Prieto AI, Guzmán-Guillén R, et al. Occurrence and toxicity of microcystin congeners other than MC-LR and MC-RR: a review. Food Chem Toxicol 2019;125:106–132.
[36] Zeisberg M, Neilson EG. Biomarkers for epithelial-mesenchymal transitions. J Clin Invest 2009;119:1429–1437.
[37] Nakanishi T, Tamai I. Roles of organic anion transporting polypeptide 2A1 (OATP2A1/SLCO2A1) in regulating the pathophysiological actions of prostaglandins. AAPS J 2018;20:13.
[38] Raska J, Ctverackova L, Dydowiczova A, et al. Tumor-promoting cyanotoxin microcystin-LR does not induce procarcinogenic events in adult human liver stem cells. Toxicol Appl Pharmacol 2018;345:103–113.
[39] Schmidt N, Mishra A, Lai GH, et al. Arginine-rich cell-penetrating peptides. FEBS Lett 2010;584:1806–1813.
[40] **Wang D**, **Yang S**, Zhao Y, et al. Identifying and validating molecular subtypes of biliary atresia using multiple high-throughput data integration analysis. Front Immunol 2023;13:1008246.
[41] Raghu G, Berk M, Campochiaro PA, et al. The multifaceted therapeutic role of N-acetylcysteine (NAC) in disorders characterized by oxidative stress. Curr Neuropharmacol 2020;19:1202–1224.
[42] Tessier MEM, Shneider BL, Brandt ML, et al. A phase 2 trial of N-Acetylcysteine in biliary atresia after Kasai portoenterostomy. Contemp Clin Trials Commun 2019;15:100370.
[43] Chatterjee S, More M. Cyanobacterial harmful algal bloom toxin microcystin and increased *Vibrio* occurrence as climate-change-induced biological co-stressors: exposure and disease outcomes via their interaction with gut–liver–brain axis. Toxins (Basel) 2023;15:289.
[44] Hopkins PC, Yazigi N, Nylund CM. Incidence of biliary atresia and timing of hepatoportoenterostomy in the United States. J Pediatr 2017;187:253–257.
[45] Wada H, Muraji T, Yokoi A, et al. Insignificant seasonal and geographical variation in incidence of biliary atresia in Japan: a regional survey of over 20 years. J Pediatr Surg 2007;42:2090–2092.
[46] Ayas MF, Hillemeier AC, Olson AD. Lack of evidence for seasonal variation in extrahepatic biliary atresia during infancy. J Clin Gastroenterol 1996;22:292–294.
[47] Wyrebek R, Fierstein JL, Wells RG, et al. A case-control study of the association between *Karenia brevis* (Red Tide) and biliary atresia. MedRxiv 2022;133:102596. https://doi.org/10.1101/2022.10.24.22279447. Published online October 26.
[48] Girard M, Jannot AS, Besnard M, et al. Polynesian ecology determines seasonality of biliary atresia. Hepatology 2011;54:1893–1894.
[49] Nakamizo M, Toyabe S, Kubota M, et al. Seasonality in the incidence of biliary atresia in Japan. Acta Paediatr 2006;95:511–512.
[50] **Cavallo L**, **Kovar EM**, Aqul A, et al. The epidemiology of biliary atresia: exploring the role of developmental factors on birth prevalence. J Pediatr 2022;246:89–94.
[51] Lee KJ, Kim JW, Moon JS, et al. Epidemiology of biliary atresia in Korea. J Korean Med Sci 2017;32:656–660.

Keywords: Algal toxins; Biliary atresia; Bile duct; Glutathione and oxidative stress; Harmful algal bloom.
Received 6 February 2024; received in revised form 3 September 2024; accepted 4 September 2024; Available online 12 September 2024